Composition, structural, and electrical properties of fluorinated silicon–nitride thin films grown by remote plasma-enhanced chemical-vapor deposition from SiF_4/NH_3 mixtures

J. Fandiño and A. Ortiz
Instituto de Investigaciones en Materiales, Universidad Nacional Autónoma de México, Ciudad Universitaria, Coyoacán 04510, México Distrito Federal, México

L. Rodríguez-Fernandez
Instituto de Física, Universidad Nacional Autónoma de México, Ciudad Universitaria, Coyoacán 04510, México Distrito Federal, México

J. C. Alonso[a]
Instituto de Investigaciones en Materiales, Universidad Nacional Autónoma de México, Ciudad Universitaria, Coyoacán 04510, México Distrito Federal, México

(Received 14 August 2003; accepted 17 February 2004; published 27 April 2004)

Fluorinated silicon–nitride films (SiN_x:F) have been prepared at 250 °C by remote plasma-enhanced chemical-vapor deposition using mixtures of SiF_4/NH_3 in different proportions. The structure, relative composition, and fluorine content of the films were evaluated by Fourier-transform infrared spectroscopy, Rutherford backscattering, ellipsometry, and resonant nuclear-reaction analysis. The electrical properties of the films were also assessed from the current–voltage characteristics of Al–SiN_x:F–Si metal–insulating–semiconductor structures. It was found that the SiF_4/NH_3 ratio produces little influence on the refractive index and density of the films, but this ratio has important effects on the fluorine content, deposition rate, and electrical properties. In general, these SiN_x:F films are free of Si–H bonds, chemically stable, and show breakdown fields above 8 MV/cm. © *2004 American Vacuum Society.* [DOI: 10.1116/1.1699335]

I. INTRODUCTION

Although silicon nitride in the form of thin film has been prepared and studied for many years,[1] its remarkable physical properties make this insulator a promising material for present and future technological applications, including solar cells,[2,3] radiative cooling,[4] resonant structures and some other micromechanical applications,[5–7] thin film transistors, etc.[8,9]

Also, the advent of submicron electronic-device fabrication has brought unprecedented interest in silicon nitride as a gate dielectric material[10,11] and intermetallic dielectric.[12] Most of these applications require the preparation of silicon–nitride thin films at low temperatures to avoid interdiffusion between adjacent layers of devices. Silicon–nitride films have been obtained at low temperatures (<350 °C) by plasma-enhanced chemical vapor deposition (PECVD) in several versions such as capacitively coupled PECVD,[13,14] electron cyclotron resonance-PECVD,[15,16] inductively coupled remote plasma enhanced chemical vapor deposition (RPECVD), etc.[17–20]

However, in spite of the intrinsic differences between the PECVD versions mentioned above, the generalized use of SiH_4 as the silicon source is a common factor that produces silicon nitrides with a substantial amount of hydrogen (20–40 at. %), in the form of Si–H and N–H bonds.[16–20] This hydrogen lowers the chemical and thermal stability, and degrades the electrical properties of the films, causing severe reliability problems when they are used in electronic devices.

In order to avoid the incorporation of hydrogen in these films, different approaches have been used, including He dilution and thermal annealing in a nitrogen ambient,[21] rapid thermal annealing,[22] plasma pretreatments,[23] and optimization of gas-source mixtures.[24] Nevertheless, the intrinsic chemistry of the SiH_4 plasma process will make further hydrogen content optimization very difficult because processing temperatures will be forced to go down by technological requirements.

Another method to overcome this problem is the addition of fluorine precursors that act as hydrogen gettering agents. For example, mixtures of $NF_3/N_2/SiH_4$ and $NF_3/NH_3/N_2/SiH_4$ have been used for depositing fluorinated silicon-nitride films at 300 °C by direct and remote PECVD.[25–27] In these cases the films that result have fluorine atoms incorporated (from 6 to 20 at. %) in their Si_3N_4 network, and for this reason they are called fluorinated silicon–nitride films. However, even at high fluorine concentrations, some Si–H bonds remain in these films, and they contain unexpectedly high oxygen concentrations.[25,26]

Another approach that has been used for reducing the incorporation of hydrogen is to change the SiH_4 gas by other silicon gaseous source, with less or none hydrogen content, such as: HMDS,[28] TDMAS,[29] and SiF_4.[30–33] In particular, the use of silicon–fluorine precursors such as SiF_4, SiF_2, or Si_2F_6 in combination with N_2 and H_2, proposed two decades ago by Fujita to obtain PECVD fluorinated silicon nitride films at 350 °C,[30–33] was demonstrated to have some advantages, such as the complete elimination of Si–H bonds from

[a]Electronic mail: alsono@servidor.unam.mx

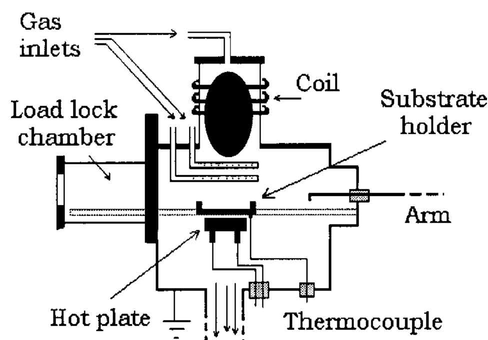

FIG. 1. Schematic diagram of the RPECVD system. The NH_3 and Ar gases are supplied from the top inlet line. The SiF_4 gas is fed downstream through one dispersal ring.

the films and an improvement in their chemical and electrical stability.

In spite of this, some important questions on these fluorinated silicon–nitride films, such as the dependence of composition, film microstructure, bonding configuration, stability, and electrical properties, with fluorine content, were no studied further and no later reports on this approach are found in the literature. Recently ultrathin fluorinated silicon–nitride gate-dielectric films have been prepared by electron cyclotron-resonance PECVD, at 350 °C using SiF_4 as a silicon source gas.[34] In that work it is shown that the control of the fluorine concentration in the films, to less than 11.5 at. %, is a key factor to obtain high quality materials at low temperatures.

However, there are no more reports on the use of SiF_4 for PECVD of silicon–nitride films, and it is worthwhile to study this matter further in order to point out its practical benefits, advantages, and limitations.

In this work, we use different SiF_4/NH_3 mixtures in an inductively coupled RPECVD reactor in order to obtain fluorinated silicon nitride films at 250 °C. We also study the dependence of film deposition rate, composition, bonding configuration, stability, and electrical properties on the fluorine content. No Si–H bonds evidence was found from Fourier-transform infrared (FTIR) spectra in the whole range of film compositions explored. Films with fluorine content up to 22 at. % show good electrical behavior and chemical stability without any postdeposition treatment.

II. EXPERIMENT

Our deposition system, schematically shown in Fig. 1, was home designed and manufactured by the company MV-Systems Inc. (Colorado, USA). Our system consists of a vacuum-deposition chamber (26 500 cm^3 total volume) which contains a boron–nitride hot plate, coupled to a proportional and integral differential temperature controller and capable to rise substrate temperatures from ambient up to 700 °C. The top part of the chamber consists of a quartz tube 4 in. in diameter and 20 cm in height. This tube is surrounded by a water-cooled copper coil, which is responsible for the power transfer from the radio frequency (rf) source (13.56 MHz) to the plasma. The turbomolecular-mechanical vacuum-pump system (Varian) of the chamber guarantees a base pressure of 10^{-6} Torr. The system also has a load-lock chamber that allows the deposition chamber to be kept in a vacuum between runs.

TABLE I. Deposition parameters.

Parameter	Value
Substrate temperature (°C)	250
Pressure (mTorr)	10
rf power (W)	550
Ar flow rate (sccm)	37
NH_3 flow rate (sccm)	7
SiF_4 flow rate (sccm)	1.5, 3.5, 7, 14

For depositing the silicon–nitride films, NH_3 and Ar gases were fed into the plasma zone of the chamber from the top end of the quartz tube. Meanwhile the SiF_4 gas was fed downstream of the plasma by means of one dispersal ring (4 in. in diameter) that lay just a few centimeters over the substrate holder. The flow rates of the gases, whose values appear in Table I, were controlled automatically by means of MKS electronic mass-flow meters. The other growth parameters were fixed at the values shown in the same table. In order to investigate the effect of the SiF_4/NH_3 flow ratio ($R=SiF_4/NH_3$) on the film properties, the only parameter that was changed from run to run was the SiF_4 flow rate (1.5, 3.5, 7.0, and 14.0 sccm). For making the structural, optical, and composition analysis, silicon–nitride films of two different thicknesses (approximately 90 and 400 nm thick, respectively) were deposited on one side of specular-polished, 350 μm thick, *n*-type (100), 200 Ω cm resistivity, crystalline–silicon substrates. These substrates were cleaned prior to deposition with semiconductor grade HF diluted in deionized water. For the fabrication of metal–insulating–semiconductor (MIS) structures, films of approximately 90 nm were deposited on *n*-type (100) single crystalline silicon substrates with lower resistivity (0.1–2 Ω cm), which were additionally cleaned following the Radio Corporation of America standard cleaning method. The deposition conditions used in this work assured good film uniformity on silicon wafers of 2 in. in diameter.

The thickness and refractive index of the films were measured *ex situ* by ellipsometric measurements, carried out by means of a null single-wavelength (632.8 nm) Gaertner L117 ellipsometer. Chemical-bonds analysis was performed using a FTIR Nicolet 210 spectrophotometer, operated in the range of 400–4000 cm^{-1}, with a 4 cm^{-1} resolution. The fluorine content in the SiN_x:F films was measured by resonant nuclear-reaction analysis (RNRA) employing the particle-gamma reaction $^{19}F(p,\alpha\gamma)^{16}O$ at a resonance energy of 340.5 keV.[35] The relative concentration for Si, N, and F in the film was obtained using Rutherford backscattering spectrometry (RBS) with 0.7 MeV $^4He^+$ ions. The ion beam impinged at normal incidence on the target and backscattered particles at 177° were detected by an annular surface-barrier detector. Those two ion-beam analysis techniques were per-

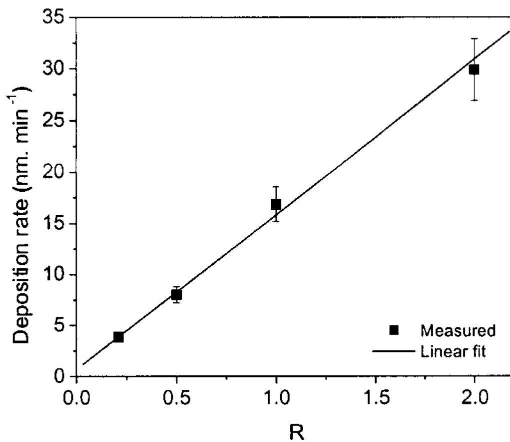

FIG. 2. Growth rate vs gas flow ratio, $R = SiF_4/NH_3$.

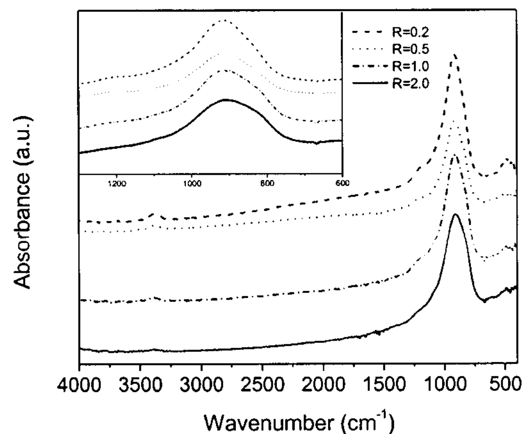

FIG. 3. Infrared absorption spectra of fluorinated silicon-nitride films as a function of $R = SiF_4/NH_3$. The inset shows in a close up, that a hump appears (around 830 cm^{-1}) in the main absorption peak as R increases.

formed using the 0.7 MeV Van de Graaff accelerator at the Instituto de Física, UNAM. Several runs per value of R were performed in order to check reproducibility.

In order to perform electrical characterization, Al/SiN_x:F/Si/(In–Ga) MIS structures were constructed with 200-nm-thick aluminum dots (0.013 cm^2 in area), which were thermally evaporated on SiN_x:F surfaces. The back-ohmic contact was manually applied from an In–Ga eutectic. No thermal anneal was made after the construction of the MIS capacitors. Current–voltage characteristics were assessed at 0.5 V s^{-1} with the aid of a Keithley 230 voltage source and a Keithley 485 picoammeter controlled through the general purpose interface bus via software.

III. RESULTS

A. Deposition rate and film composition

Figure 2 shows the deposition rate of the films as a function of the SiF_4/NH_3 flow-rate ratio $R = SiF_4/NH_3$. It must be pointed out that the deposition rate, defined as the ratio of film thickness to deposition time, was similar for both thin (~90 nm) and thick (~400 nm) films. It can be seen from Fig. 2 that the deposition rate increases linearly as R increases. No saturation effect in the deposition rate was observed in the range of the SiF_4 flow rates investigated.

In Fig. 3 the infrared absorption smoothed spectra of films (~400 nm thick) deposited under the different SiF_4 flow rates are shown. All the spectra show a major and broad absorption band centered at approximately 914 cm^{-1} which can be associated to stretching vibrations of Si–N bonds in fluorinated silicon nitride films.[30,33] In the close-up of the spectra (see inset of Fig. 3), it is seen that this band broadens and a small hump appears around 830 cm^{-1} as R increases. The bonding configuration of fluorine atoms cannot be identified easily from these infrared (IR) spectra because the three absorption peaks associated to vibrations of Si–F_x ($x = 1,2–3,4$) bonds, which occur around 828, 930, and 1110 cm^{-1}, respectively,[36,37] as well as the absorption peak associated to N–F bonds occurring at 1032 cm^{-1},[33] are practically veiled by the broad Si–N absorption peak. Each spectrum of Fig. 3 also shows some absorption features at 3384 and 1210 cm^{-1}, which are related to stretching and bending N–H bonds, respectively, and whose intensities decrease as R increases. As can be seen from the spectra of Fig. 3, there are no absorption peaks related to Si–H bonds (2150–2250 cm^{-1}),[25,38–40] which indicates that, if they exist, the amount is below FTIR detectable level (~0.5%–1% for thick films).[40–42] The absorption band that occurs in the IR spectra between 430 and 525 cm^{-1} could be attributed to a-Si atom breathing vibrations.[37,39] However, this feature can also have a contribution of Si–N breathing mode vibrations (480–490 cm^{-1}).[43,44] Anyway, the behavior of this absorption band with the changes in R is neither clear nor reliable because the spectra in this region were too noisy before smoothing and these spectra had base lines with different slopes.

Because there were no Si–H bonds found in the films, the hydrogen content was calculated by integrating the N–H stretching absorption peak, using the formula

$$C_H = A \int \frac{\alpha(\nu)}{\nu} d\nu, \tag{1}$$

where α is the absorption coefficient and A is a proportionality factor equal to 2.8×10^{20} cm^{-2} for N–H bonds.[19] Although this equation gives the absolute H concentration in the films (cm^{-3}), using the RBS data for the atom density it was possible to convert this concentration into the relative hydrogen atomic percentage concentrations shown in Fig. 4.[45] It was found that the H percentage concentration decreases from around 20 to 9 at. % as R increases from 0.2 to 2.0.

The atomic concentration of F, Si, and N incorporated in the films were obtained from RBS measurements. The Si/N ratio obtained from RBS measurements, as a function of R, is plotted in Fig. 4. Taking into account the error bars, this ratio is nearly constant (Si/N≈1) for $R = 0.25–1.0$ and increases slightly (Si/N≈1.2) as $R = 2.0$. Considering that the ratio Si/N in our films is larger than that for the stoichiometric nitride, Si_3N_4 (Si/N=0.75), all of them can be defined as silicon rich nitrides. From the RBS measurements we did not find any evidence of bulk oxygen in the films. On the other

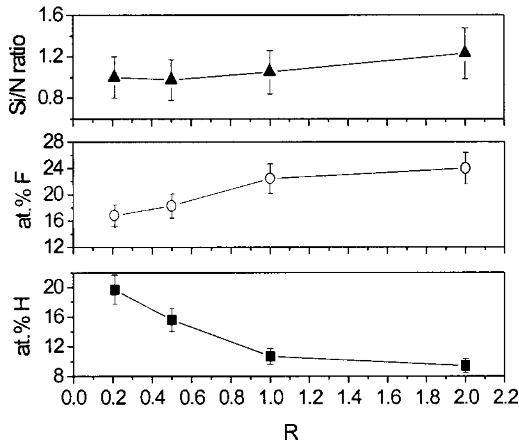

FIG. 4. Si/N ratio (▲), at. % F (○), and at. % H (■) as a function of R for fluorinated silicon nitride films deposited by RPECVD from $SiF_4/NH_3/Ar$ mixtures.

hand, the fluorine concentrations determined from RBS were in perfect agreement with those values obtained by means of RNRA. The concentration of fluorine atoms incorporated in the SiN_x:F films as a function of R, determined from RNRA and RBS, is also shown in Fig. 4. As expected, fluorine content increases as R rises, and in this case it ranges between 17 and 24 at. % which is higher than the values previously reported in the literature for SiN_x:F films.[26,27,34] The RNRA spectra from which the fluorine content in the films was measured are shown in Fig. 5. From the flatness of these experimental curves in the region between 345 and 370 keV it is concluded that the fluorine distribution is nearly uniform in all the films. It is interesting to note from Fig. 4 that the sum %F+%H is nearly constant (36%–33%) for all the values of R, which suggests that these elements are mutually excluded.

B. Refractive index and density

The behavior of refractive indices of the deposited films as a function of R is illustrated in Fig. 6. It can be observed that the refractive indices of our fluorinated silicon–nitride films are (in general) lower than those for stoichiometric silicon–nitride films ($n=2.0$) and they decrease slightly (from 1.71 to 1.67) as R increases from 0.2 to 2.0. Accurate

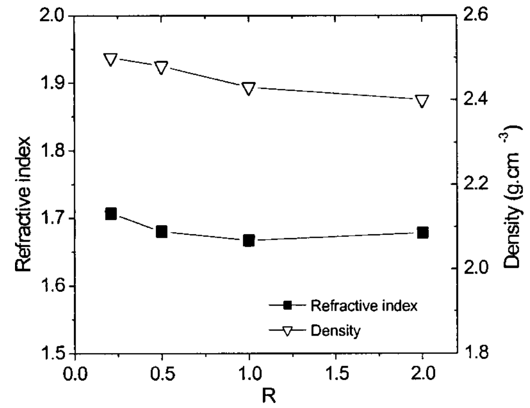

FIG. 6. Refractive index and density of films as a function of R.

film thickness measurements (provided by ellipsometric instrumentation) together with RBS data were used in order to obtain information about film densities. Figure 6 also shows the effect of R variations on the density of the films. Similarly to the behavior of the refractive index, there is only a slight decrease in the density (from 2.5 to 2.4 gr cm^3) of the films as R increases in the whole range studied.

C. Electrical properties

Figure 7 shows the typical current–voltage characteristics of MIS structures incorporating SiN_x:F films deposited under the various investigated values of R. The leakage current densities for samples prepared with $R=0.2$ and 0.5 are quite low (below 1×10^{-7} A/cm^2), including for electric fields as high as 6 MV/cm. For the sample prepared with $R=1.0$ the leakage current increases in approximately one order of magnitude and the sample prepared with $R=2.0$ suffers a drastic increase in the leakage current (more than three orders of magnitude). In spite of the degradation in the leakage current as R increases, all the samples exhibit electrical-breakdown

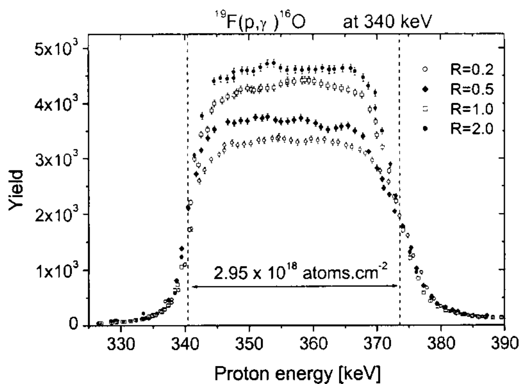

FIG. 5. RNR spectra from which the fluorine content in the silicon nitride films was measured, as a function of R.

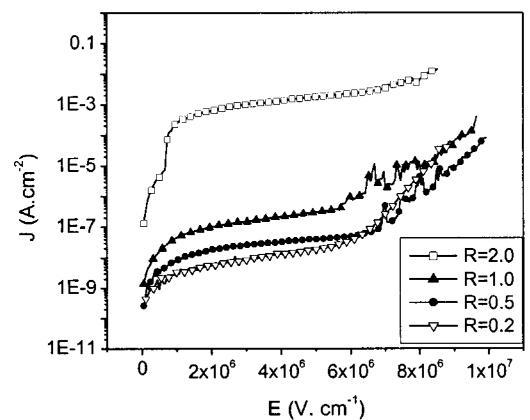

FIG. 7. Current density–electric field characteristics for MIS structures fabricated with fluorinated silicon nitride films deposited at 250 °C with different R.

fields higher than 8.5 MV/cm. However, as Table III shows there was no clear trend in the breakdown field as a function of R.

IV. DISCUSSION

A. Deposition process, film composition, and bonding configuration

The behavior of the deposition rate shown in Fig. 2 can be explained by the growth models generally accepted for the RPECVD process of silicon compounds.[18,46,47] According to these models, in our specific case, it can be assumed that the growth rate r_D of the SiN_x:F films correlates directly with the gas-phase density of the nitrogen species $[NH_y]^*$ ($y=0,1,2$) generated from the excitation of the NH_3 in the plasma zone, and also with the concentration of silicon species $[SiF_z]$ ($z=0$, 1, 2, 3) produced downstream of the plasma. Under this scheme, the formation of the silicon nitride films can be understood in terms of the overall reaction

$$([NH_3])^* + [SiF_4] \rightarrow [NH_y] + [SiF_z] \rightarrow a\text{-}SiN_x\text{:F,H}, \quad (2)$$

where the asterisk denotes that the NH_3 gas is plasma excited, and $[SiF_z]$ is the concentration of SiF_z radicals generated downstream of the plasma by the impact of the NH_y plasma-excited species with the SiF_4 molecules. At this point, it must be clarified that for the sake of simplicity fluorinated silicon–nitride films are usually denoted as SiN_x:F, however, sometimes they are denoted as in the Eq. (2), SiN_x:F,H, in order to explicit the fact that they may contain an important amount of hydrogen.

Since the Ar metastables and electrons (and possibly energetic Ar ions) generated in the plasma zone move downstream, and can excite and break the SiF_4 molecules, it is possible to have additional parallel reactions between silicon fluorine radicals such as

$$([Ar] + [e])^* + [SiF_4] \rightarrow [SiF_z] + [SiF_w] \rightarrow a\text{-Si:F}, \quad (3)$$

($z,w=0$, 1, 2, 3) which can give rise to the formation of an amorphous fluorinated-silicon constituent in the film.

Since in our RPECVD processes all the deposition parameters were kept constant, except the SiF_4 flow rate, and the amount of reactive SiF_x species must be proportional to this flow rate, it is expected that the deposition rate increase linearly with the flow rate of the SiF_4 precursor (see Fig. 2). The relatively low deposition rate of these fluorinated silicon nitride films, compared with those films deposited from SiH_4 and NH_3 or NF_3,[25–27] among other things, can be attributed to the high energy required for dissociation of SiF_4 into neutral SiF_z radicals (minimum threshold energy ~10.8 eV),[48] compared to that required for dissociation of SiH_4 into neutral SiH_z radicals (minimum threshold energy ~8 eV).[49]

The formation of the SiN_x:F,H compound can be explained in terms of radical addition reactions among the NH_y ($y<3$) and SiF_z ($z<4$) radicals, which form Si–N bonds that give rise to a solid deposit and gaseous byproducts such as F, F_2, H, HF, etc. Since fluorine and hydrogen atoms come naturally bonded to the SiF_4, and NH_3 precursors, respectively, the remaining of Si–F and N–H bonds in the film

TABLE II. Strengths of some chemical bonds.

Bond	Energy (kcal mol^{-1})	Reference
N–F	73.3	50
Si–H	74.7, 71.51	50, 51
N–H	85.9, 81.0	50, 51
Si–N	112.3	51
Si–F	129.0, 131.9	50, 51
H–F	135.8	50

network is well expected. Thus it is plausible that the solid deposit be formed by combinative bonding of multibonded units such as F–Si–N–H, F_2–Si–N–H, F_2–Si–N–H_2, etc. giving rise to the composition denoted by SiN_x:F,H. Based on the parallel reaction pathway given by Eq. (3), it is also possible the formation of fluorinated silicon–silicon bonds such as F–Si–Si–F, etc. Finally, the composition of the resulting film will be determined by the type of radicals generated in the RPECVD process, the rate of production and concentration of these radicals, and the relative chemical reaction rates among them.

Although the previous simplified model cannot explain completely the composition of the films, besides explaining the incorporation of fluorine and hydrogen in the silicon–nitride films, it is consistent with most of our experimental results and tendencies observed. For example, the presence of N–H bonds in the films is clearly evidenced in all the IR spectra of Fig. 3. The increase in the amount of F incorporated in the films and the fact that the films become silicon richer as R increases (see Figs. 4 and 5), can be explained on the basis of this model. If the film grows from additive reactions among the NH_y ($y<3$) and SiF_z ($z<4$) radicals, it is clear that as $R=SiF_4/NH_3$ increases, there will be a larger concentration of SiF_z radicals than NH_x radicals for film deposition, and consequently more silicon and fluorine atoms, in comparison with nitrogen and hydrogen atoms, will be incorporated into the film. This can also explain the decrease in the concentration of N–H bonds as R increases and why the sum of %F+%H remains nearly constant (see Figs. 3 and 4).

The presence of Si–F bonds cannot be easily evidenced from the IR spectra because the absorption peaks associated to these bonds are veiled by the broad Si–N absorption peak, however, the appearance of the small hump at around 830 cm^{-1} as R increases (see inset of Fig. 3), seems to be indicative of their existence, since this wavelength corresponds to vibrations of Si–F bonds.

Additionally, the assumption that the SiN_x:F,H films grow from reactions among radicals having Si–F and N–H native bonds, along with the fact that the bonding energy of Si–H is lower than that of N–H, Si–N, and Si–F (see Table II), makes less probable the incorporation of Si–H bonds in the films.[26,27,30,33] This explains the fact that Si–H bonds do not appear in any of the IR spectra (at least up to the FTIR detection limit, ~1%). Since the bonding energy of N–F is even lower than that of Si–H (see Table II), based on similar arguments, the incorporation of N–F bonds in the films is

less probable. On the other hand because the H–F bonds are thermodynamically more stable than the Si–F and N–H bonds (see Table II), it is probable that F and H atoms be removed from their parent radicals (SiF_z and NH_y), and join each other to form volatile HF. We believed that this mutual F and H abstraction mechanisms enhances the formation of Si–N bonds.

The fact that the Si/N ratio in the films changes much more slowly (from 1.0 to 1.23) than the SiF_4/NH_3 ratio (from 0.2 to 2.0) in the feed gases is not well understood at present. However, the explanation could be related to the high thermochemical stability or lower reactivity of the SiF_4 molecules compared with that of the NH_3 molecules. On the other hand, in our RPECVD process the NH_3 and Ar gases, whose flow rates were constant, are dissociated and excited in the plasma region, meanwhile the SiF_4 is fed downstream of the plasma and therefore it is basically dissociated by encounters with NH_y radicals and Ar metastables coming from the plasma region. Thus, it is expected that the incorporation of silicon in the films be little sensitive to changes in the SiF_4 flow rate.

B. Refractive index and density

As Fig. 6 shows, we found low values and near-insensitive behavior (a very small decrease) in the refractive index of our films as R changed by one order of magnitude. These results are in agreement with the values and behavior of refractive indices reported for fluorinated silicon–nitride films deposited from fluorinated-silicon sources (SiF_4 and SiF_2).[30,31,33] However, they are in contrast with those results reported for hydrogenated silicon nitride films deposited by PECVD from the SiH_4/NH_3 mixtures.[19,27,25] In the latter cases the refractive index can be considerably varied (from 1.8 to 2.5) because it depends basically of the Si/N ratio of the film. So, for these silicon nitride films an increase in the SiH_4/NH_3 ratio above a certain value produces silicon rich compositions ($Si/N>1$) which give rise to high refractive index values, closer to that of hydrogenated amorphous silicon (3.4).[52] In the case of fluorinated silicon nitride films, the refractive index not only depends on the Si/N ratio, but also on the fluorine content. The low values of refractive index obtained for fluorinated silicon nitrides have been attributed to the incorporation of fluorine.[25–27,30,33] Although the reasons for this reduction have not been well studied yet, it can be speculated that they are similar to that for the lower refractive index of fluorinated SiO_2 films.[27,53] The hypotheses adapted to silicon nitride films are the following: (1) fluorine incorporation (probably in the form of Si–F bonds) reduces the electronic polarizability of the silicon nitride matrix because the electronegativity of fluorine is higher than that of Si and N atoms, (2) fluorine abstracts and reduces (and even eliminate) the concentration of more polarizable constituents such as Si–H, and consequently lowers or eliminate this contribution to the refractive index, and (3) fluorine incorporation leads to a less dense film because the Si–F bonds are terminal and separate the fundamental SiN_4 tetrahedral that form the ideal Si_3N_4 network. It is worth mentioning that the last hypothesis is consistent with the low density found in our films (see Fig. 6). On this premise, the small changes in the refractive index of our fluorinated silicon nitride films (see Fig. 6) can be explained as a result of the combination of two opposite effects. One of these is the increment in the refractive index, produced by the increase in the Si/N ratio as a consequence of increasing the ratio, $R=SiF_4/NH_3$. This effect is similar to that occurring for films deposited from the SiH_4/NH_3 mixtures. The opposite effect is the reduction in the refractive index due to the higher incorporation of fluorine atoms in the films, as R increases. Thus, the quasicompensation of these opposite effects, with a slight predomination of the latter, can give rise to the small decrease in the refractive index shown in Fig. 6. In consistence with the previous discussion, some authors have been able to increase the refractive index of fluorinated silicon nitride films to get values equal to that of the stoichiometric material (2.0), or even higher (2.5), using $SiH_4/N_2/NF_3$ plasmas.[26,27] In order to achieve this, they use very low flow rates of NF_3 (or high SiH_4/NF_3 ratio) to reduce the fluorine content and to increase the Si/N ratio. However, under these conditions hydrogen is incorporated in the film network in the form of Si–H bonds, in concentrations high enough to be clearly detected in the IR spectra.

The behavior of film density as a function of R observed in Fig. 6 can be explained as follows. The densities of our films (between 2.4 and 2.5 g/cm^3) are lower than the density of the stoichiometric Si_3N_4 material (3.1 g cm^{-3}). However, these densities are consistent and even slightly higher than that of SiN_x:H (2.38 g/cm^3) and SiN_x:F (2.2–2.42 g/cm^3) films, which were plasma deposited from SiH_4/NH_3 and SiH_4/NF_3 mixtures, respectively.[26,27] The reduction in the density of both hydrogenated and fluorinated films, compared with that of the stoichiometric material is well expected, if it is assumed that each hydrogen or fluorine atom enters in the ideal Si_3N_4 network as a terminal Si–H, N–H, or Si–F bond, separating the SiN_4 tetrahedra originally joined by Si–N bonds. The separation of the SiN_3H or SiN_3F tetrahedra tends to open the structure, which produces the consequent reduction in the film density. On the other hand, if some remaining Si dangling bonds link with each other to form Si–Si bonds, there will be an additional density reduction, because the Si–Si bond length (~2.34 Å) is larger than the original Si–N bond length (~1.87 Å).[54] The small reduction found in the density of our films as R increases can be again explained in terms of opposite effects that almost cancel each other. In one effect, for the reasons described previously, as R increases the incorporation of Si–F tends to decrease the density of the films. However, the incorporation of Si–F produces also an opposite effect that tends to increase the density of the films, because the Si–F bond length (~1.54 Å)[54] is lower than the Si–N bond length and the mass of F is higher than the mass of N. Additionally the reduction in the amount of N–H bonds that occurs when R increases favors the joining of SiN_4 tetrahedra though the formation of Si–N bonds, which also produce an incremental increase in film density.

TABLE III. Breakdown fields as a function of R for MIS structures incorporating fluorinated silicon–nitride films deposited at 250 °C.

R	E_B (MV cm^{-1})
0.2	8.8
0.5	9.9
1.0	9.6
2.0	8.5

C. Electrical properties

It has been commonly observed that Si-rich silicon–nitride films deposited from SiH_4/NH_3 mixtures exhibit high leakage currents when used as gate insulators.[55] The reason for these poor electrical properties has been attributed not only to the low values of the N/Si ratios, but also to the presence of hydrogen in the films, in the form of weak Si–H bonds. This becomes the main limitation for expanding the applications in microelectronic devices. However, the J vs E plots of our MIS capacitors shown in Fig. 7 reveal relative low values of current densities and high breakdown fields when R remains below 2. This finding means that under these conditions, our films, in spite of being silicon rich (Si/N ratios as high as 1.05), have good electrical integrity. We believe that our films have more flexibility in the Si/N ratios because they do not have Si–H bonds, and instead they have stronger Si–F bonds. The fact that the better electrical properties correspond to films with high H concentrations in the form of N–H bonds reinforce the criteria that N–H bonds are not responsible for insulating degradation in SiN_x:H films.

Poole–Frenkel (P–F) emission has been established as the main bulk-limited electron conduction mechanism in silicon–nitride insulators.[1] In order to investigate whether this is the dominant mechanism present in our films, we plotted $\ln(J/E)$ vs $E^{1/2}$ for high electric fields (close to electric breakdown). The linearity of the $\ln(J/E)$ vs $E^{1/2}$ plots for high electric fields (close to electric breakdown), and the values of the dynamic permittivities (which are close to 5.5 in all the cases), that we obtained from these plots, indicate that P–F emission could be the main bulk-limited electron-conduction mechanism in our silicon–nitride films. In this case, it has been proposed in the literature that the cause of the increment in the leakage current of silicon nitride films is the reduction in the P–F barrier height as the films become Si rich.[55] We believe that fluorine incorporation in the film network contributes to enhance the barrier height because fluorine incorporation serves as a passivating agent against trap centers generated by Si dangling bonds. Also, the absence of Si–H bonds, which are commonly found in PECVD silicon nitride films deposited from SiH_4, eliminates a great amount of deep traps. The high values of E_B obtained for all our samples, as Table III shows, is attributed to the stronger nature of Si–F bonds with respect to Si–H and Si–N bonds. The increase in the leakage current that is observed in our films as R increases, in spite of the expected beneficial effect of fluorine incorporation, is not well understood at present. However, one possible explanation is that the increase in the amount of Si–Si bonds, relative to the amount of Si–N bonds, as R increases, means that the insulating electrical properties of the fluorinated silicon nitride films tend to have a electrical behavior more similar to that of the a-Si:F semiconductor.

D. Chemical stability

After being exposed to the ambient humidity at room temperature, the chemical stability of our SiN:F films was studied through measurements of the refractive index and FTIR spectra. After exposure to ambient for a period of 3 months, there was no oxidation effect observed in the samples nor a change in any of the parameters measured in any sample. This allows to conclude that all the films are stable when exposed to the ambient environment. The stability of our samples, in spite of the high fluorine concentrations (between 17 and 24 at. %), confirms that these fluorinated silicon–nitride films do not contain weak Si–H bonds, and that fluorine atoms are probably incorporated in the films, forming strong Si–F bonds in the monofluoride configuration.

V. CONCLUSIONS

Fluorinated silicon–nitride films (SiN_x:F) were prepared at low temperature (250 °C) by RPECVD using mixtures of SiF_4 and NH_3, and the effect of the ratio of these gases (R) on the physical and chemical properties of the films has been examined. It was found that R has a little effect on the refractive index and density of the films, but large variations took place these films' deposition rate, composition, and electrical properties when R varied from 0.2 to 2. Analysis of FTIR spectra performed on as-deposited films in the whole composition range allows us to conclude that all these films are free of Si–H bonds. In spite of the fact that fluorinated silicon–nitride films that were plasma deposited from this chemistry have high fluorine concentrations (17–24 at. %), as indicated by RNRA and RBS analysis, these films show good chemical stability and high resistance to oxidation under exposure to the ambient moisture. The chemical stability, along with the compositional analysis data, suggest that the fluorine incorporation in these films occurs by substituting nitrogen atoms in the silicon–nitride network. That is to say, some Si–N bonds are substituted for stronger Si–F bonds.

All the MIS capacitors constructed with these fluorinated silicon–nitride films meet quite well the low-temperature processing requirement for microelectronics and show breakdown fields above 8 MV cm^{-1}. Films deposited with $R<2$ have leakage current densities lower than 1×10^{-6} A/cm^2.

ACKNOWLEDGMENTS

The authors would like to thank S. Jiménez, M. A. Canseco, L. Huerta, and J. Camacho from the Instituto de Investigaciones en Materiales, and Rafael Macías and J. C. Pineda from the Instituto de Física, UNAM for technical assistance. This work has been supported by Consejo Nacional de Ciencia y Tecnología (CONACyT) of México under Project No. 26423-A.

[1] S. M. Sze, J. Appl. Phys. **38**, 2951 (1967).
[2] A. Rohatgi, P. Doshi, J. Moschner, T. Lauinger, A. G. Aberle, and D. S. Ruby, IEEE Trans. Electron Devices **47**, 987 (2000).
[3] I. O. Parm *et al.*, Sol. Energy Mater. Sol. Cells **74**, 97 (2002).
[4] Z. Liang, Sol. Energy **72**, 505 (2002).
[5] L. Sekaric, D. W. Carr, S. Evoy, J. M. Parpia, and H. G. Craighead, Sens. Actuators, A **101**, 215 (2002).
[6] R. Kressmann, M. Klaiber, and G. Hess, Sens. Actuators, A **100**, 301 (2002).
[7] D. Memmi, V. Foglietti, E. Cianci, G. Caliano, and M. Pappalardo, Sens. Actuators, A **99**, 85 (2002).
[8] Y. Kuo, Vacuum **51**, 741 (1998).
[9] D. Stryahilev, A. Sazonov, and A. Nathan, J. Vac. Sci. Technol. A **20**, 3143 (1997).
[10] Q. Lu *et al.*, IEEE Electron Device Lett. **22**, 324 (2001).
[11] K. M. Chang, C. C. Cheng, and C. C. Lang, Solid-State Electron. **46**, 1399 (2002).
[12] M. Vogt, M. Kachel, K. Melzer, and K. Drescher, Surf. Coat. Technol. **98**, 948 (1998).
[13] J. Bandet, B. Despax, and M. Caumont, J. Appl. Phys. **85**, 7899 (1999).
[14] V. Gottschalch, R. Schmidt, B. Rheinlander, D. Pudis, S. Hardt, J. Kvietkova, G. Wagner, and R. Franzheld, Thin Solid Films **416**, 224 (2002).
[15] S. Matsuo and M. Kiuchi, Jpn. J. Appl. Phys., Part 2 **22**, L210 (1983).
[16] M. C. Hugon, F. Delmotte, and B. Agius, J. Vac. Sci. Technol. A **15**, 3143 (1997).
[17] G. Lucovsky, P. D. Richard, D. V. Tsu, S. Y. Lin, and R. J. Markunas, J. Vac. Sci. Technol. A **4**, 681 (1986).
[18] G. Lucovsky, D. V. Tsu, and R. J. Markunas, in *Handbook of Plasma Processing Technology*, edited by M. Rossnagel, J. J. Cuomo, and W. D. Westwood (Noyes, Park Ridge, NJ, 1990).
[19] Y. B. Park and S. W. Rhee, J. Mater. Sci.: Mater. Electron. **12**, 515 (2001).
[20] Y. Ma, T. Yasuda, and G. Lucovsky, Appl. Phys. Lett. **64**, 2226 (1994).
[21] S. V. Hattangady, G. G. Fountain, R. A. Rudder, and R. Markunas, J. Vac. Sci. Technol. A **7**, 570 (1989).
[22] C. Boehme and G. Lucovsky, J. Appl. Phys. **88**, 6055 (2000).
[23] M. Bose, D. K. Basa, and D. N. Bose, Mater. Lett. **48**, 336 (2001).
[24] C. Doughty, D. C. Knick, J. B. Bailey, and J. E. Spencer, J. Vac. Sci. Technol. A **17**, 2612 (1999).
[25] C. P. Chang, D. L. Flamm, D. E. Ibbotson, and J. A. Mucha, J. Appl. Phys. **62**, 1406 (1987).
[26] C. S. Pai, C. P. Chang, F. A. Baiocchi, and J. Swiderski, J. Appl. Phys. **68**, 2242 (1990).
[27] B. H. Jun, J. S. Lee, and D. W. Kim, J. Mater. Res. **14**, 995 (1999).
[28] N. I. Fainer, Y. M. Rumyantsev, M. L. Kosinova, G. S. Yurjev, E. A. Maximovskii, and F. A. Kuznetsov, Appl. Surf. Sci. **113/114**, 614 (1997).
[29] T. Aoki *et al.*, Vacuum **51**, 747 (1998).
[30] S. Fujita, H. Toyoshima, T. Ohishi, and A. Sasaki, Jpn. J. Appl. Phys., Part 2 **23**, L144 (1984).
[31] S. Fujita, H. Toyoshima, T. Ohishi, and A. Sasaki, Jpn. J. Appl. Phys., Part 2 **23**, L268 (1984).
[32] S. Fujita, T. Ohishi, H. Toyoshima, and A. Sasaki, J. Appl. Phys. **57**, 426 (1985).
[33] S. Fujita and A. Sasaki, J. Electrochem. Soc. **135**, 2566 (1988).
[34] H. Otha, M. Hori, and T. Goto, J. Appl. Phys. **90**, 1955 (2001).
[35] J. P. Hirvonen, in *Handbook of Modern Ion Beam Material Analysis*, edited by J. R. Tesmer and M. Nastasi (Material Research Society, Pittsburgh, 1995).
[36] C. J. Fang, L. Ley, H. R. Shanks, K. J. Gruntz, and M. Cardona, Phys. Rev. B **22**, 6140 (1980).
[37] K. Yamamoto, M. Tsuji, K. Washio, H. Kasahara, and K. Abe, J. Phys. Soc. Jpn. **52**, 925 (1983).
[38] A. C. Adams, Solid State Technol. **26**, 135 (1983).
[39] D. V. Tsu and G. Lucovsky, J. Vac. Sci. Technol. A **4**, 480 (1986).
[40] G. Lucovsky and D. V. Tsu, J. Vac. Sci. Technol. A **5**, 2231 (1987).
[41] V. Pankov, J. C. Alonso, and A. Ortiz, J. Appl. Phys. **86**, 275 (1999).
[42] J. A. Theil, D. V. Tsu, M. W. Watkins, S. S. Kim, and G. Lucovsky, J. Vac. Sci. Technol. A **8**, 1374 (1990).
[43] S. Fujita, H. Toyoshima, and A. Sasaki, J. Appl. Phys. **64**, 3481 (1988).
[44] M. Lattemann, E. Nold, S. Ulrich, H. Leiste, and H. Holleck, Surf. Coat. Technol. **174/175**, 365 (2003).
[45] A. C. Adams, in *VLSI Technology*, edited by S. M. Sze (McGraw-Hill, New York, 1988), pp. 262–266.
[46] M. J. Kushner, J. Appl. Phys. **63**, 6538 (1993).
[47] J. C. Alonso, E. Pichardo, L. Rodríguez-Fernández, J. C. Cheang-Wong, and A. Ortiz, J. Vac. Sci. Technol. A **19**, 507 (2001).
[48] T. Nakano and H. Sugai, J. Phys. D **26**, 1909 (1993).
[49] M. J. Kushner, J. Appl. Phys. **74**, 2532 (1988).
[50] R. T. Sanderson, *Chemical Bonds and Bond Energy*, 2nd ed. (Academic, New York, 1976).
[51] J. A. Kerr and D. W. Stockes, in *Handbook of Chemistry and Physics*, 83rd ed., edited by D. R. Lide (Academic, New York, 2002).
[52] G. D. Cody, in *Semiconductors and Semimetals*, edited by J. I. Pankove (Academic, Orlando, 1984) Vol. 21, Part B, p. 20.
[53] S. M. Hang and E. S. Aydil, J. Appl. Phys. **83**, 2172 (1998).
[54] F. A. Cotton, G. Wilkinson, and P. L. Gauss, *Basic Inorganic Chemistry*, 3rd ed. (J Wiley, New York, 1995), p. 97.
[55] S. Habermehl and C. Carmignani, Appl. Phys. Lett. **80**, 261 (2002).